A gain-of-function RAC2 mutation is associated with bone marrow hypoplasia and an autosomal dominant form of severe combined immunodeficiency

Chantal Lagresle-Peyrou,[1,2,3] Aurélien Olichon,[4] Hanem Sadek,[3] Philippe Roche,[5] Claudine Tardy,[4] Cindy Da Silva,[3] Alexandrine Garrigue,[3] Alain Fischer,[2,6,7] Despina Moshous,[6] Yves Collette,[5] Capucine Picard,[2,6,8,9] Jean Laurent Casanova,[2,6,10,11,12] Isabelle André[1,2] and Marina Cavazzana[1,2,3]

[1]Laboratory of Human Lymphohematopoiesis, INSERM UMR 1163, Imagine Institute, F-75015 Paris, France; [2]Paris Descartes University – Sorbonne Paris Cité, Imagine Institute UMR1163, F-75015 Paris, France; [3]Biotherapy Clinical Investigation Center, Groupe Hospitalier Universitaire Ouest, Assistance Publique-Hôpitaux de Paris, INSERM CIC 1416, F-75015 Paris, France; [4]Cancer Research Center of Toulouse, CRCT, University of Toulouse, UPS, INSERM U1037, F-31037 Toulouse, France; [5]Marseille Cancer Research Center, CRCM, Aix Marseille University, Institut Paoli-Calmettes, CNRS, INSERM, Team ISCB, F-13273 Marseille, France; [6]Department of Pediatric Immunology, Hematology and Rheumatology, Necker-Enfants Malades University Hospital, APHP, F-75015 Paris, France; [7]College de France, F-75231 Paris, France; [8]Study Center for Primary Immunodeficiencies, Assistance Publique–Hôpitaux de Paris (AP-HP), Necker-Enfants Malades University Hospital, F-75015 Paris, France; [9]Laboratory of Lymphocyte Activation and Susceptibility to EBV, INSERM UMR 1163, Imagine Institute, F-75015 Paris, France; [10]Laboratory of Human Genetics of Infectious Diseases, Necker Branch INSERM UMR 1163, Imagine Institute, F-75015 Paris, France; [11]St. Giles Laboratory of Human Genetics of Infectious Diseases, Rockefeller Branch, Rockefeller University, New York, NY, USA and [12]Howard Hughes Medical Institute, New York, NY, USA

©2021 Ferrata Storti Foundation. This is an open-access paper. doi:10.3324/haematol.2019.230250

Received: June 20, 2019.

Accepted: January 8, 2020.

Pre-published: January 9, 2020.

Correspondence: *MARINA CAVAZZANA* - m.cavazzana@aphp.fr

CHANTAL LAGRESLE-PEYRO - chantal.lagresle@inserm.fr

Supplementary METHODS

Construction and production of the lentiviral vectors. The backbone of the replication-defective, self-inactivating pWPI lentiviral vector was provided by Addgene (https://www.addgene.org/). All the constructs (G12R, G12V, D57N and E62K) were generated by GenScript (https://www.genscript.com). Lentiviral supernatants were produced by the vector facility at SFR BioSciences Gerland-Lyon Sud (Lyon, France) and used at a multiplicity of infection of 20 or 80 for HEK and CD34+ cells, respectively. All procedures with genetically modified cells were approved by the French National Biotechnology Council and the French Ministry of Research (reference: 4983/3).

Live cell imaging analyses on fibroblasts.

For holotomography analyses, the cell sample was seeded into a 35-mm glass bottom-dish (Ibidi-Dishes™ # 81156; Ibidi, GmbH) and placed into the viewing area of the 3D Cell Explorer microscope, a live cell imaging microscope (Nanolive SA). The refractive index was measured within the cell (i.e. label-free visualization of cellular organelles) and the images were processed using STEVE software (Nanolive).

For the proliferation assays, fibroblasts were seeded into 24-well plates (10 000 cells/well, 3 wells/group) and cultured for 6 days at 37°C, 5% CO2. Cyto Tox green reagent-4632 (Essen BioSience, Ann Arbor, MI, USA) was added in the culture. To evaluate the proliferation curves and cell death, each well were photographed every 6 h (IncuCyte, Essen, MI, USA) during 6 days. The analyses were performed using IncuCyte ZOOM software (Essen BioScience).

Cord blood (CB) CD34+ cell culture

CB CD34+ HSPCs were cultured as previously described [1] and transduced with the appropriate vector. The transduction efficiency (percentage of GFP+ cells) was measured after two days on a Gallios flow cytometer,

and the data processed using Kaluza software (Beckman Coulter). The CD34+ cells' ability to differentiate in vitro along the granulocyte or T cell lineage was measured as described elsewhere [2,3].

Flow cytometry, Mitotracker DILC1(5) and CellRox staining

Monoclonal antibodies against CD7(MT-701), CD11b (D12), CD34 (8G12), and mouse IgG1k, IgG2a and IgG2b isotype controls, and the reagents annexin V and 7-aminoactinomycin D (7AAD) were obtained from BD Biosciences (San José, CA). CD15 (80H5) and mouse IgM control antibodies were purchased from Beckman Coulter (San Diego). The mitochondrial membrane potential was measured using a MitoProbe™ DILC1(5) assay kit (M34151, Thermo Fisher Scientific). The cation cyanine dye DILC1(5) passively penetrates into the cells and accumulates in mitochondria with active polarized membrane potential. A decreased staining indicate a disruption of mitochondrial membrane potential. Staining with annexin V and 7-AAD are also added during the staining to, respectively, measure apoptosis and remove the dead cells. The CellROX® Deep Red assay kit (C10492, Thermo Fisher Scientific) is used to detect the production of hydroxyl radical, a Reactive Oxygen Species (ROS), in live cells. The reagents become brightly fluorescent upon oxidation. SYTOX® Blue Dead Cell staining is also added to performed the analysis only on gated live cells (SYTOX negative). Cell analysis was performed on a Gallios flow cytometer.

G-LISA® RAC Activation assay and immunoblots on the HEK293T cell line.

To detect the amount of captured active RAC2 with the G-LISA-RAC2 assay, 10 µg/ml of the RAC2 specific antibody (AT2G11, sc-517424.) and 1/2000 HRP-conjugated anti-mouse antibody (#1721011) were used. The reaction was visualized by the addition of 100 µl of chromogenic substrate (1-step UltraTMB, 34028, Thermo Scientific) for 3 min, and stopped with 50 µl H2SO4 1N. Absorbance at 450 nm was measured using FLUOstar OPTIMA microplate reader. Whole cell extracts were obtained by lysing cells in G-LISA lysis buffer supplemented with a protease inhibitor cocktail. Proteins were separated by SDS-PAGE, and immunoblotted with anti-RAC2 (AT2G11, sc-517424, Santa Cruz Biotechnology, Inc.) or anti GAPDH (14C10, Cell

Signaling Technology) antibodies. Immunoblots were revealed by chemiluminescence using the ChemiDoc MP System (Bio-Rad). Protein levels were quantified with Image Lab software.

Supplemental table 1 : hematological analysis of bone marrow aspirate

	Blasts (%)	**PMN** (%)	**Proerythroblasts** (%)	**Lymphocytes (%)**	**Megacaryocytes**
Normal values (1 month)	0-2	10-30	0-2	10-15	present
P1 (7 days*)	11	1	rare	rare	rare
P2 (23 days*)	2	0	1	rare	rare
P3 (30 days*)	rare	absent	rare	absent	absent

PMN : Polymorphonuclear neutrophil

* age at the time of the bone marrow aspirate

Supplementary figure 1

a

```
Rac2    MQAIKCVVVG DGAVGKTCLL ISYTTNAFPG EYIPTVFDNY SANVMVDSKP VNLGLWDTAG QEDYDRLRPL SYPQTDVFLI CFSLVSPASY
Rac1    MQAIKCVVVG DGAVGKTCLL ISYTTNAFPG EYIPTVFDNY SANVMVDGKP VNLGLWDTAG QEDYDRLRPL SYPQTDVFLI CFSLVSPASF
Rac3    MQAIKCVVVG DGAVGKTCLL ISYTTNAFPG EYIPTVFDNY SANVMVDGKP VNLGLWDTAG QEDYDRLRPL SYPQTDVFLI CFSLVSPASF
                   G1                  Switch I    G2                  G3          Switch II

Rac2    ENVRAKWFPE VRHHCPSTPI ILVGTKLDLR DDKDTIEKLK EKKLAPITYP QGLALAKEID SVKYLECSAL TQRGLKTVFD EAIRAVLCPQ
Rac1    ENVRAKWYPE VRHHCPNTPI ILVGTKLDLR DDKDTIEKLK EKKLTPITYP QGLAMAKEIG AVKYLECSAL TQRGLKTVFD EAIRAVLCPP
Rac3    ENVRAKWYPE VRHHCPHTPI LLVGTKLDLR DDKDTIERLR DKKLAPITYP QGLAMAREIG SVKYLECSAL TQRGLKTVFD EAIRAVLCPP
                                G4                                                  G5

Rac2    PTRQQKRACSLL
Rac1    PVKKRKRKCLLL
Rac3    PVKKPGKKCTVF
```

b

	G12R Score	damaging score
SIFT	0.002	<0.05
Polyphen *(Human variation)*	0.67	> 0.5
CADD	28	>15
EXAC/ Z score	3.16	> 3

c

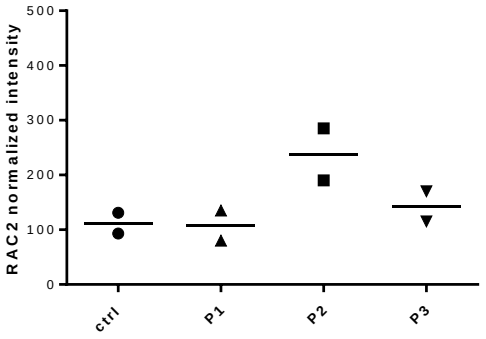

d

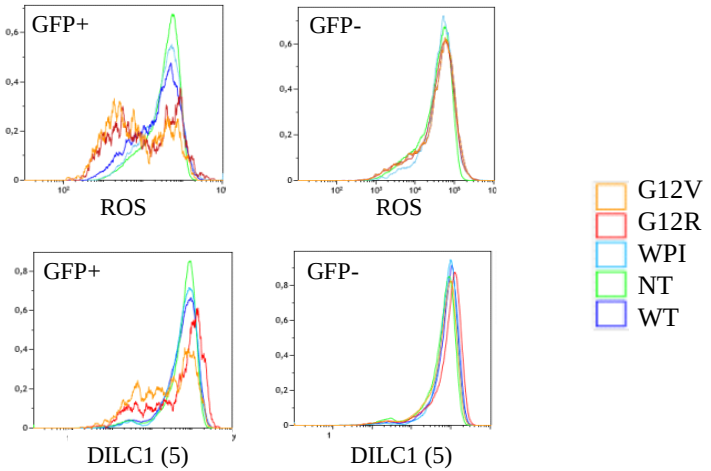

e

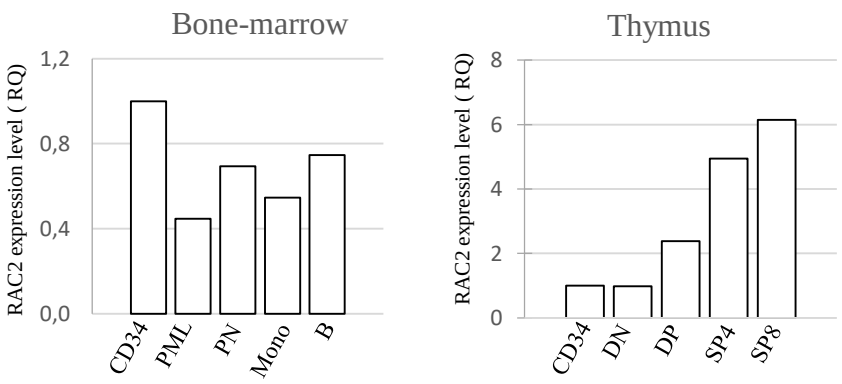

Supplementary Figure 1:

a. Site of the G12R mutation.

A schematic representation of RAC1, RAC2 and RAC3 GTPase sequences (adapted from Olson et al [4]). The highly conserved G boxes (G1 to G5) are represented by green squares, and the switch I and switch II regions are represented by blue squares. Amino acids affected by the missense mutation described in the present study (p.G12R) are depicted in bold and red. Bold and underlined amino acids represent other previously described missense mutations (the p.P34H and p E62K GOF mutations, and the p.D57N LOF mutation).

b. Prediction of the impact of the G12R mutation, according to various *in silico* tools.

The fig shows the score for the G12R mutation and the score thresholds for damaging mutations, according to the Sorting Intolerant from Tolerant (SIFT), Polymorphism Phenotyping (Polyphen), Combined Annotation Dependent Depletion (CADD), and Exome Aggregation Consortium (Exac) tools.

c. RAC2 protein expression

Two immunoblots of RAC2 protein expression in lysates from control fibroblasts (Ctrl) and fibroblasts derived from the affected individuals (P1, P2 and P3). Each dot represents one experiment. The quantification was performed with the LiCor Odyssey system using GAPDH as the loading control to normalized RAC2 expression intensity.

d. Flow cytometry analysis of DILC and ROS staining on proliferative HSPCs .

Flow cytometry assays of ROS production (cellRox) and mitochondrial membrane depolarization (DILC1(5)) in the GFP+ and GFP- live cells gates for the five conditions: G12V- (orange), G12R- (red), WT- (dark blue), WPI- (blue) transduced cells and non-transduced cells (green).

d. Quantification of RAC2 mRNA levels in human bone marrow haematopoietic cells and thymocytes.

The samples were sorted by flow cytometry in order to separate: CD34+ progenitors (CD34), CD15+CD11b- promyelocytes (PMLs), CD15+CD11b+ polynuclear neutrophils (PN), CD14+CD11b+ monocytes (Mono) and CD19+ B-cell (B) for the bone marrow cells; CD4-CD8- double-negative (DN), CD4+CD8+ double-positive (DP) and CD3+CD4+ T-cells (SP4) or CD3+CD8+(SP8) cells (for the thymocytes). Total RNA was reverse-transcribed using random hexamers and MultiScribe MuLV reverse transcriptase (Applied Biosystems). RT-PCR on cDNA was performed with the endogenous GAPDH (Hs00266705) and RAC2 (Hs 00427439) probes labelled with 6-carboxy-fluorescein dye (Applied Biosystems). All reactions were performed using an ABI Prism 7900 sequence detection system (Applied Biosystems). The data were analysed using the comparative cycle threshold method and expressed as the relative quantification (RQ) of RAC2 expression level with GAPDH as the endogenous control and CD34 as the calibrator sample (CD34). The data are representative of two independent experiments with triplicate wells for each experiments.

Supplementary figure 2

a

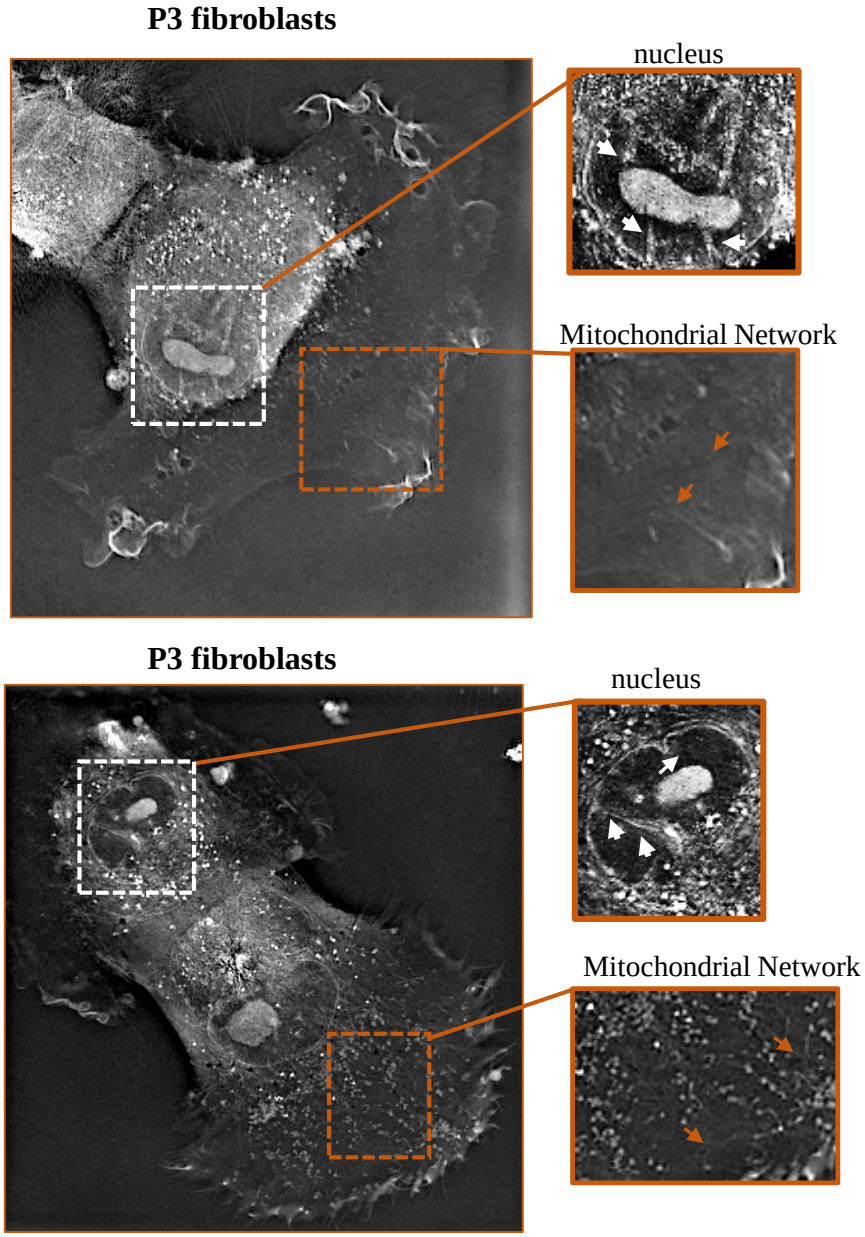

b

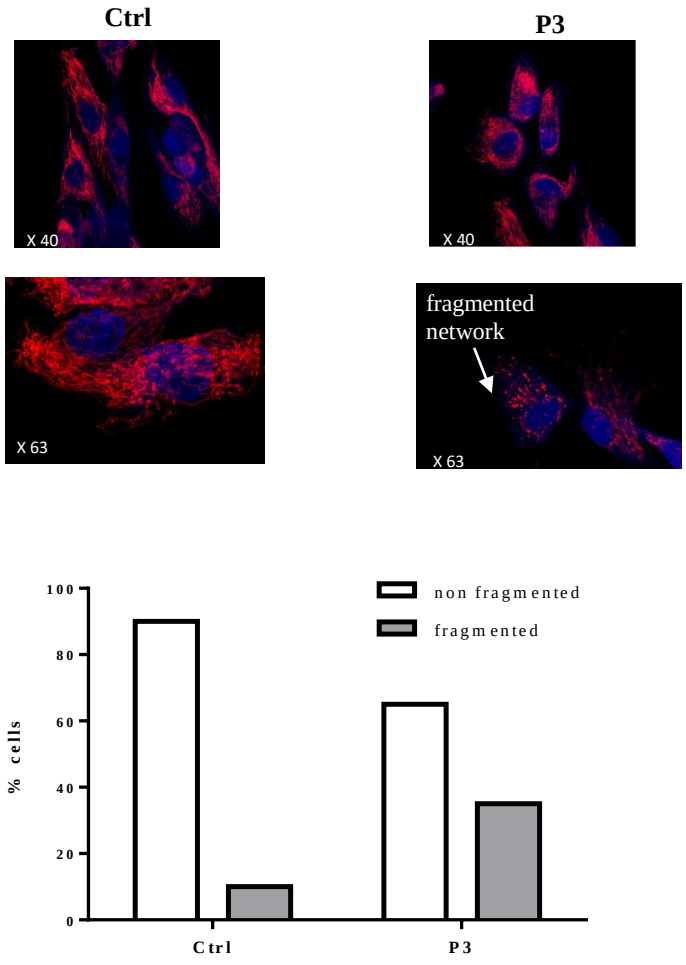

Supplementary figure 2 :

a. Live cell imaging of P3 fibroblasts.

The analyses were performed with a 3D Cell Explorer microscope using holomomography technology. Cultures of P3 fibroblasts are shown. White arrows indicate the nuclear envelope and brown arrows the mitochondrial network. Scale bar =10 mm, 1 pixel= 0.188um..

b. Fluorescence microscopy images showing cellular distribution of mitochondria in fibroblasts from control (ctrl) or patient (P3)

Upper panel : Slides section of fibroblasts were stained with MitoTracker Deep Red (red staining, In vitrogen, M7512) and Dapi (blue staining, In vitrogen, P36931). Confocal microscopy analyses were performed with a Zeiss confocal microscope (SP8 STED) and images were processed using Fiji software.
Lower panel : The mitochondrial network was analysed on individual fibroblast (n = 242 cells counted for control in two independent experiments and n=170 cells counted for P3 control in two independent experiments) with the quantification method described elsewhere [5]

Supplementary figure 3

a

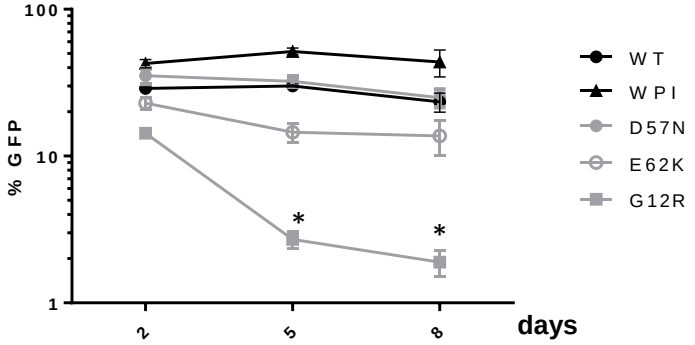

b

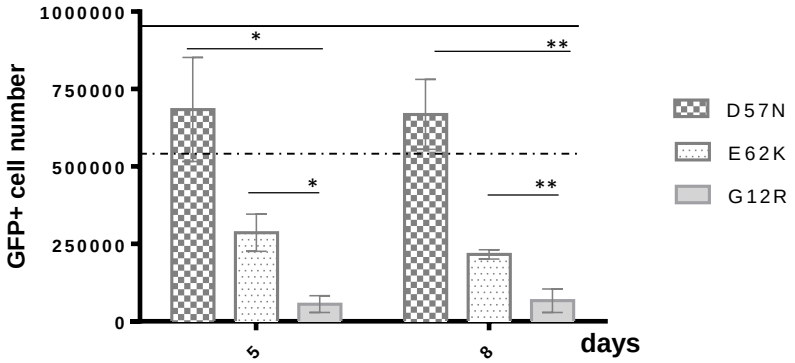

c

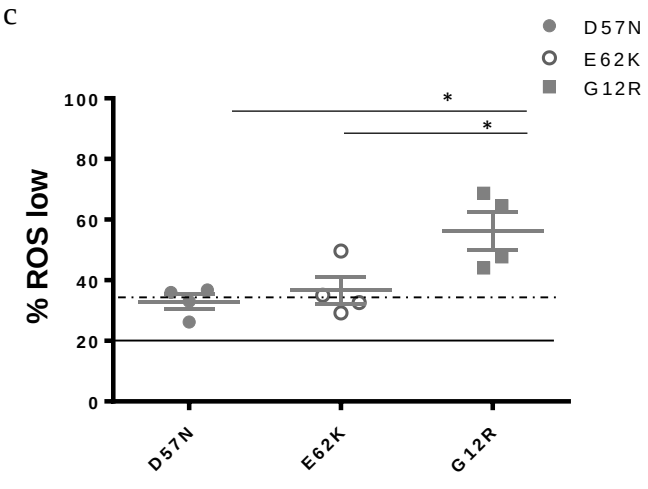

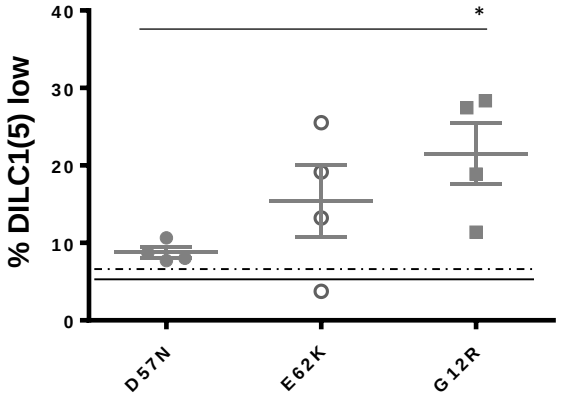

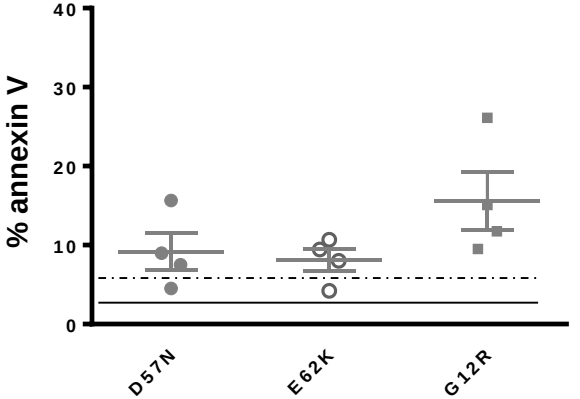

d

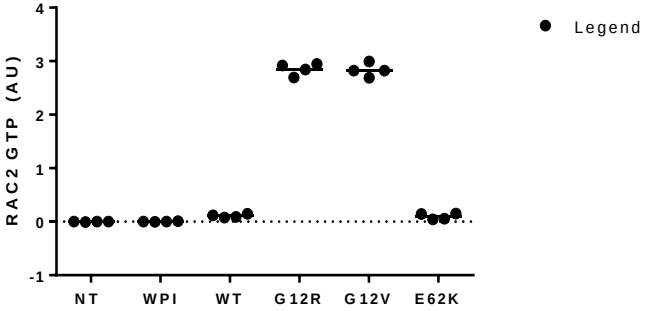

% GFP (1)	92	88	84	88	85
% GFP (2)	83	83	69	69	71

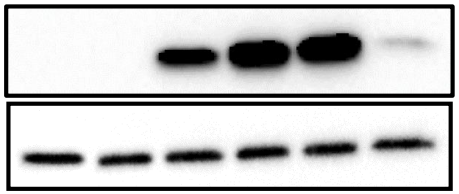

Ratio RAC2/GAPDH				
	1	2,09	2,44	0,088

Supplementary Figure 3:

a and b. Impact of the G12R, D57N and E62K mutations on HSPCs proliferation
The proliferation of transduced $CD34^+$ cells was measured in an 8-day culture. Flow cytometry was used to analyse (a) the change over time in the percentage of GFP+ cells from day 2 (when the transduction efficiency is measured) until day 7 (end of the culture) and (b) the number of GFP-expressing cells. All the analyses were performed in the live cell (7-AAD-negative) gate. The dotted line and the full line represent the median values for the WT and pWPI conditions, respectively. The results are The results are quoted as the mean ± SEM and are representative of four independent experiments. *$p<0.05$; **$p<0.01$

c. Impact of the G12R, D57N and E62K mutations on mitochondrial membrane potential and ROS production
The respective proportions of ROS-low, DILC1(5)-low and annexin V+ cells (as a percentage of the GFP+ live cells) were analyzed on day 4. The dotted line and the plain line represent the median values for the WT and pWPI conditions, respectively. The results are representative of four independent experiments. *$p<0.05$

d. RAC2 GTP activity and total RAC2 expression in HEK293T cells
HEK293T cells were either not transduced (NT, control) or were transduced with a lentiviral empty vector (WPI) containing the wild type (WT) form of *RAC2* cDNA, the mutated form described here (G12R) or (as a positive control) the constitutively activated RAC2 GTP form (G12V). Two days after transduction, flow cytometry was performed to measure the the percentage of GFP+ expressing cells (%) in each condition. Cells were recovered for analysis with the G-LISA assay (15 µg total protein per well) and immunoblotting (25 µg total protein input per well). The quantification of the GTP-bound RAC2 form (RAC2 GTP) is quoted as the mean of two independent determinations. The immunoblotting results are representative of two independent experiments (1 and 2).

Supplemental Video M1 : **A gain-of-function RAC2 mutation is associated with bone marrow hypoplasia and an autosomal dominant form of severe combined immunodeficiency**

Cell live imaging using the 3D Cell Explorer microscope (Nanolive SA) was performed on control fibroblasts (left panel) and P3 fibroblast (right panel). Acquisition time : each minute during 12 hours.

References

1- Lagresle-Peyrou C, Six EM, Picard C, et al. Human adenylate kinase 2 deficiency causes a profound hematopoietic defect associated with sensorineural deafness. Nat Genet 2009;41(1):106–111.

2- Six E, Lagresle-Peyrou C, Susini S, et al. AK2 deficiency compromises the mitochondrial energy metabolism required for differentiation of human neutrophil and lymphoid lineages. Cell Death Dis 2015;6e1856.

3- Reimann C, Six E, Dal-Cortivo L, et al. Human T-lymphoid progenitors generated in a feeder-cell-free Delta-like-4 culture system promote T-cell reconstitution in NOD/SCID/γc(-/-) mice. Stem Cells 2012;30(8):1771–1780.

4 - Olson MF. Rho GTPases, their post-translational modifications, disease-associated mutations and pharmacological inhibitors. Small GTPases 2018 ; 9 : 203-215.

5 - Olichon A. et al. OPA1 alternate splicing uncouples an evolutionary conserved function in mitochondrial fusion from a vertebrate restricted function in apoptosis. Cell Death and Differentiation 2007; 14: 682–692.